σ = distribution coefficient or Henry's Law constant relating concentration of toluene in liquid to equilibrium concentration of toluene in membrane
σ_o = pre-exponential factor in Equation (9)
θ = lag time in Equation (8)
div = divergence
grad = gradient

Subscripts

L = left side of membrane
R = right side of membrane

LITERATURE CITED

1. Chandler, H. W., and E. J. Henley, *AIChE J.*, **7**, 295 (1961).
2. Long, R. B., *Ind. Eng. Chem. Fundamentals*, **4**, 445 (1965).
3. McCall, D. W., *J. Polymer Sci.*, **26**, 151 (1957).
4. Zhookhovitzky, A. A., *Intl. J. Appl. Radiation Isotopes*, **5**, 159 (1959).
5. Gromov, B. A., *ibid.*, **13**, 281 (1962).
6. deBrouchers, L., R. von Lumpert, and R. Stein, *Proc. Conf. Radioisotopes Phys. Indus.*, 187, Copenhagen (1960).
7. Symonds, A. E., *U.S. At. Energy Comm. Rept. DP-792* (1963).
8. Barrer, R. M., "Diffusion In And Through Solids," Macmillan, New York (1941).
9. Barrer, R. M., and G. Skirrow, *J. Polymer Sci.*, **3**, 549 (1948).
10. McCall, D. W., *ibid.*, **26**, 151 (1957).
11. Hildebrand, J. H., and R. L. Scott, "The Solubility Of Non-electrolytes," 3rd Ed., Reinhold, New York (1950).
12. Barrer, R. M., *Trans. Faraday Soc.*, **35**, 644 (1939).
13. ———, *J. Chem. Soc.*, 278 (1934).
14. Kwei, T. K., and W. Arnheim, *J. Chem. Phys.*, **37**, 1900 (1962).
15. ————, *J. Polymer Sci.*, **2A**, 957 (1964).
16. Eyring, H., *J. Chem. Phys.*, **4**, 283 (1936).
17. Swab, G. M., *Adv. Catalysis* **2**, 251 (1950).
18. Sosnovsky, H. M. C., *J. Phys. Chem. Solids*, **10**, 304 (1959).
19. Michaels, A. S., and H. J. Bixler, *J. Polymer Sci.*, **50**, 393 (1961).

Manuscript received January 12, 1968; revision received February 23, 1968; paper accepted February 26, 1968.

Vaporization at the Base of Bubbles of Different Shape During Nucleate Boiling of Water

N. B. HOSPETI and R. B. MESLER

The University of Kansas, Lawrence, Kansas

Differently shaped bubbles were observed growing during nucleate boiling of water at atmospheric pressure. The surface temperature beneath the bubbles was measured simultaneously with a fast response surface thermocouple. The evaporation from the base necessary to account for the observed cooling was calculated. A comparison of the ratio of vapor volume formed at the base to the total volume of the bubble shows a dependency on bubble shape. The ratio is smallest for spherical bubbles, largest for hemispherical and intermediate for oblate bubbles.

Although nucleate boiling is widely used in modern technology it is still not a well understood phenomenon. A fundamental understanding demands a better knowledge of the bubbles which so clearly characterize nucleate boiling.

In the last few years it has been shown clearly that significant evaporation occurs beneath the bubbles. This evaporation has been named microlayer vaporization. This work was undertaken to determine how much of bubble volume is due to evaporation at the base and whether the amount of microlayer vaporization is a function of bubble shape. Water boiling at atmospheric pressure was studied.

Moore and Mesler (*13*) measured surface temperature fluctuations in nucleate pool boiling of water at atmospheric pressure using a fast response surface thermocouple (*9*). They found that the surface temperature occasionally dropped 20 to 30°F. in about 2 msec. This indicated a rapid extraction of heat during a short time. They postulated that the surface was cooled during initial bubble growth by evaporation of a microlayer into the bubble. Rogers and Mesler (*15*) experimentally showed that the surface temperature drops only when a bubble grows over the fast response surface thermocouple (*9*). Almost at the same time Hendricks and Sharp (*4*) and Bonnet, et al. (*1*) carried out similar work and obtained additional support for this hypothesis. Bonnet, et al. made some preliminary calculations on two bubbles formed on a stainless steel surface. They showed that about 98% of the total vapor generated in these bubbles came from the vaporization at the base of the bubbles. Cooper and Lloyd (*2*) have reported on the evaporation of a microlayer beneath toluene bubbles on a glass surface.

N. B. Hospeti is with Shell Chemical Co., Houston, Texas.

METHOD OF STUDY

The preliminary data for this study was a high-speed motion picture of bubbles growing on a surface instrumented with a fast response surface thermocouple. The thermocouple signal was photographically recorded superimposed on the bubble pictures. From such data both the bubble growth rate and the rate of heat transfer beneath the bubble can be evaluated.

If the measured surface temperature was considered to be the surface temperature of a semi-infinite solid the heat

flux at the surface could be determined by numerically solving the heat conduction equation

$$\frac{\partial^2 T}{\partial x^2} = \frac{1}{\alpha}\frac{\partial T}{\partial t} \tag{1}$$

subject to the following boundary conditions:

$$T(o, t) = f(t) \tag{2}$$

$$T(x, o) = 0 \tag{3}$$

$$T(\infty, t) = 0 \tag{4}$$

The assumption of the semi-infinite solid is justified in that heat flows from a depth in the surface which is small in comparison with surface dimensions of the area over which heat transfer is occurring.

Assuming that the cooling beneath bubbles is due to microlayer vaporization the thickness evaporated was estimated from the quantity of heat removed per unit area. The total heat removed per unit area was obtained by subtracting the enthalpy at any time from the initial enthalpy taken for convenience as zero.

$$Q/A = -C_p \rho \int_o^\infty T \, dx \tag{5}$$

The corresponding microlayer thickness evaporated is

$$M_T = \frac{Q}{A \lambda \rho_L} \tag{6}$$

obtained by integrating the rate per unit area over the base. Since the temperature and thus the heat flux is known at only one position the heat flux was assumed constant over the base to permit the integration. Actually evaporation begins at the center and proceeds outward as contact diameter increases, but this was ignored in the present treatment. This procedure predicts a uniform thickness for the microlayer evaporated for which there is experimental support. Hospeti and Mesler (5) concluded that the microlayer was uniform in thickness from the uniformity of calcium sulfate deposits formed by evaporation of the microlayer.

One estimate of bubble volume was obtained from the motion picture film assuming that the bubble was an ellipsoid with two axes equal to the maximum width of the bubble, A, and the other axis equal to the height, B. Rehm (14) showed that bubbles are bodies of revolution under similar conditions.

$$V_B = \frac{\pi}{6} A^2 B \tag{7}$$

For convenience in making comparisons an equivalent radius, R, was defined as the radius of a sphere with the same volume

$$R = \tfrac{1}{2} \sqrt[3]{A^2 B} \tag{8}$$

Also, for convenience in making comparison, the thickness of microlayer, M_B, that would have to evaporate to account for the total bubble volume, was computed by dividing the volume of liquid required by the contact area of the bubble.

$$M_B = \frac{\frac{\pi}{6} A^2 B \frac{\rho_V}{\rho_L}}{\frac{\pi}{4} C^2} = \frac{2}{3}\frac{A^2 B}{C^2}\frac{\rho_V}{\rho_L} \tag{9}$$

Note that

$$\frac{M_T}{M_B} = \frac{V_T}{V_B} = F \tag{10}$$

where V_T represents the volume of vapor produced by evaporation of the microlayer and F is the fraction of the bubble volume accounted for by microlayer vaporization.

The contribution of microlayer vaporization to bubble volume, V_T, was estimated as the product of the thickness of the microlayer and the contact area between the bubble and the surface. The contact area reaches a maximum after the fast initial growth. At the same time microlayer vaporization appears essentially complete. Therefore V_T was considered to have its final value at the time of maximum bubble contact.

It was of interest to compute the ratio of the final value of V_T to both the bubble volume at maximum contact and at departure. These ratios were taken as F_1 and F_2, respectively. For these ratios an improved estimate of bubble volume was made from measurements of bubble width, D, as a function of height, z:

$$V_B' = \frac{\pi}{4}\int_o^B D^2 \, dz \tag{11}$$

One reason for the importance of F_2 is the significance it has in the latent heat transport mechanism. Latent heat transport is defined as the quantity of heat carried away from a boiling surface by the latent heat of the vapor generated prior to bubble detachment.

EXPERIMENTAL PROCEDURE

The surface temperature was sensed by a fast response thermocouple of the type described by Kovacs and Mesler (9). It consisted of a 5 mil Alumel wire insulated with aluminum oxide and installed in a Chromel tube by drawing the tube through a 25 mil die. The thermocouple assembly was mounted in a Chromel strip ¼ × 1/16 × 1 in. which had been molded in Bakelite. The thermocouple assembly was cut off flush with the surface and polished. A tiny scratch which bridged over the aluminum oxide served as the junction. The surface was again polished to minimize the chance of the scratch serving as an artificial nucleation site.

A schematic diagram of the overall equipment is shown in Figure 1. A 750 w. a.c. light source was used to illuminate the bubbles. The fast response surface thermocouple output was fed to the oscilloscope with a high sensitivity a.c. preamplifier. The pulse generator gave 1 kc. pulses, which were amplified by the pulse shaper. The pulse shaper could control the width of the pulse from 10 to 100 μsec. This pulse was used to blank the oscilloscope trace. The timing indications obtained on the film by this blanking technique were usually much sharper than those obtained with timing lights in the camera.

A dual lens Fastax WF-17 high speed movie camera was used to photograph the bubbles and the oscilloscope trace. Both the lenses were of 2 in. focal length. The magnification, obtained by these lenses, was varied from 1:8 to 1:1 by means of a set of extension tubes ¼ to 2 in. in length. Framing rates of about 5,000 frames/sec. were used.

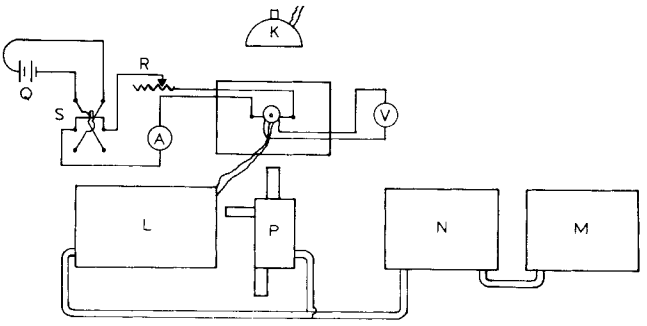

Fig. 1. Schematic drawing of the overall equipment. A. D.C. ammeter; K. A.C. light source, L. oscilloscope, M. pulse generator, N. pulse shaper, P. Fastax high speed movie camera, Q. set of 2 v. batteries, R. water cooled resistor, S. double pole switch, V. voltmeter (0-3 v.).

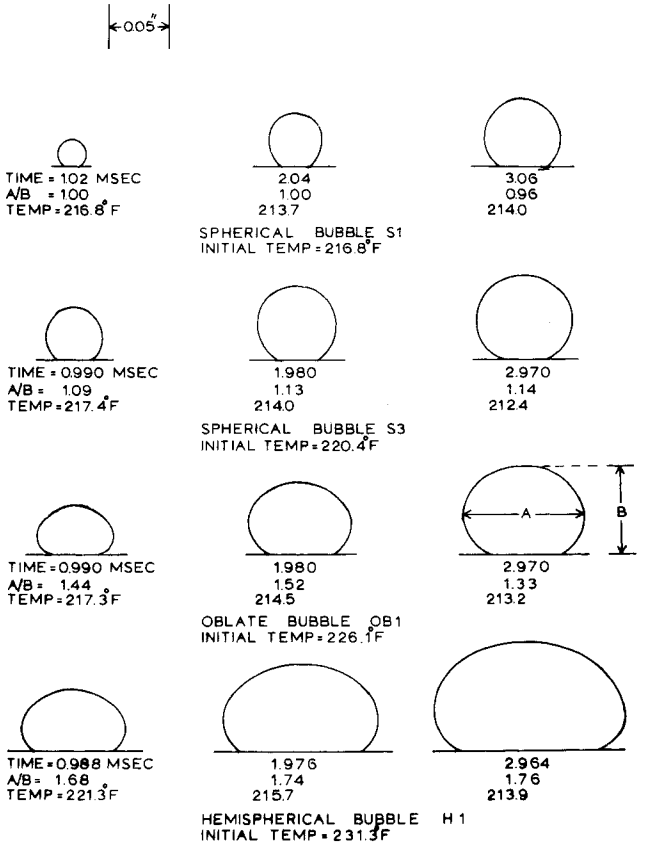

Fig. 2. Bubbles of different shapes.

A set of four batteries, 2 v. each, were used to heat the strip. The batteries were connected to the strip through a double pole switch capable of carrying 200 amps., a water cooled variable resistor and a precision ammeter. The switch was used to reverse the direction of current through the strip to measure the average surface temperature at the thermocouple. The thermocouple voltage was read on a potentiometer with the current flowing in both directions. Averaging the two readings cancelled a small voltage caused by current heating the surface. The voltage drop across the strip was measured by means of a 0-3 v. voltmeter. A more detailed description of the experimental procedure and set-up is given elsewhere (*7*).

The fluid boiled was always demineralized water from a mixed bed demineralizer. The pressure was atmospheric. The water temperature was maintained at saturation with two immersion heaters.

RESULTS AND DISCUSSION

Table 1 shows the heat flux and average temperature difference at which the six films were obtained.

A few typical bubbles were selected from the high-speed films for detailed analysis. Five spherical bubbles, ten oblate bubbles and one hemispherical bubble were analyzed.

Table 1. Heat Flux and Average Temperature Difference Data

Film no.	Heat flux B.t.u./hr. sq. ft.	$(\Delta T) = T_S - T_B$ °F.	Strip no.
32	16,000	4.5	8
33	18,000	3.0	8
34	22,000	13.0	9
35	21,000	15.3	9
36	22,000	13.0	9
37	25,000	15.0	9
W5*	63,000	26.0	—

* Donald Williams' Film no. 5, specimen 2, vertical orientation.

Due to the discontinuous nature of a framing camera the image of the bubble is recorded only at discrete time intervals. Thus, the time at which the bubble diameter is zero, or zero time is unknown. An arbitrary time scale was selected where time zero was assigned to the last vacant frame before the bubble appears on the film. Radius of the bubble, R, vs. this arbitrary time was plotted. The smooth curve of R vs. t was extrapolated to zero R at which point time was assigned to be zero. The arbitrary time scale was now shifted such that $t = 0$ coincides with $R = 0$. Similar techniques were used by other authors (*3, 8, 17, 19*).

It was observed during some preliminary experimental work, that the surface temperature dropped to saturation temperature in most of the temperature drops, for nucleate boiling of water at atmospheric pressure and saturation temperature. Moore (*12*) also observed the same phenomena. This characteristic of these temperature drops was used to set absolute values to the surface temperatures, which was essential for the comparison of surface temperatures from one film to another. This procedure was necessary because an a.c. amplifier was used to amplify the thermocouple signal for display on the oscilloscope. The minimum surface temperature for film 32 was during the oblate bubble OB1 (see Figure 5) at $t = 5$ msec. Setting this temperature at 212°F., the saturation temperature, the initial surface temperature for this bubble will be above 212 by the amount of the temperature drop at 5 msec. (212 + 14.1 = 226.1°F.). Using this basis the initial temperatures for other bubbles in film 32 were obtained. Similar procedure was adopted for other films.

Classification of Bubble Shape

Studying the shapes of bubbles during their initial growth Johnson, de la Pena, and Mesler (*8*) catalogued the shapes as spherical, oblate, and hemispherical. Spherical bubbles were reported to be the slowest growing, hemispherical the fastest, and oblate intermediate. Surface tension was shown to be dominant in spherical bubbles and inertial forces dominant in hemispherical bubbles. With oblate bubbles neither force dominated.

The effect of surface temperature on bubble shape has been reported by Hospeti and Mesler (*6*) who studied bubble growth in water under subatmospheric pressure. A lower surface temperature at the start of bubble growth produced a slower growth rate and a spherical shape. Higher temperature produced a faster growth rate and a hemispherical shape. Oblate shapes and intermediate growth rates were produced by intermediate temperatures.

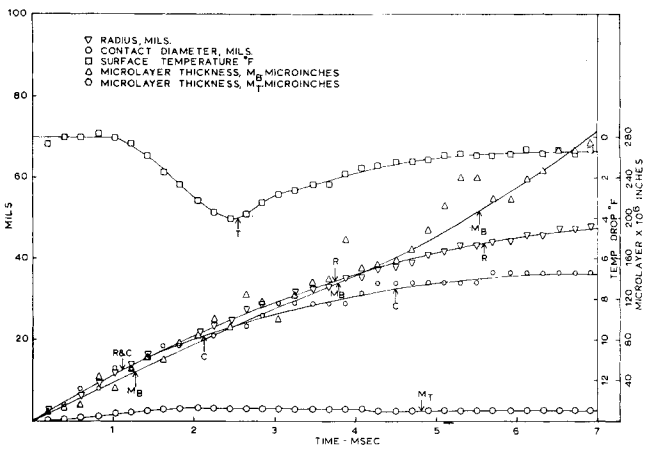

Fig. 3. Plots of radius (R), contact diameter (C), surface temperature (T) and microlayer thickness M_B and M_T for spherical bubble S1.

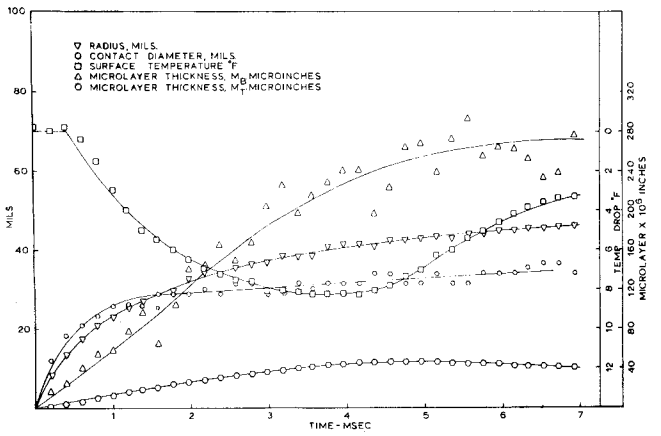

Fig. 4. Plots of radius (R), contact diameter (C), surface temperature (T) and microlayer thickness M_B and M_T for spherical bubble S3.

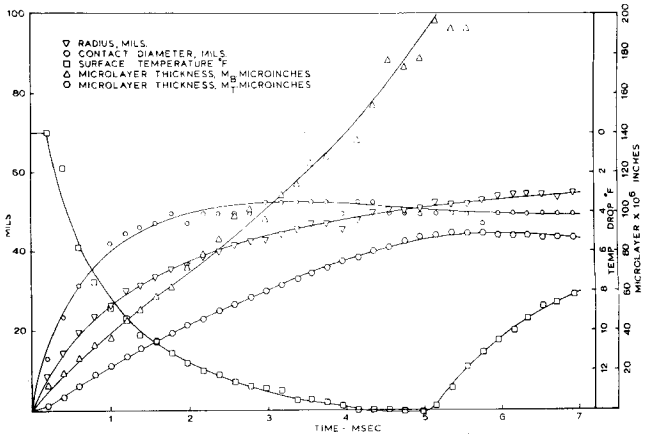

Fig. 5. Plots of radius (R), contact diameter (C), surface temperature (T) and microlayer thickness M_B and M_T for oblate bubble OB1.

Classification of shapes between spherical and oblate shapes or oblate and hemispherical shapes is aided by adopting a somewhat arbitrary criterion. The ratio of the maximum bubble width (A) to its height (B) was used. An A/B ratio of 1.0 to 1.4 was classified spherical, 1.4 to 1.7 oblate and 1.7 to 2.0 hemispherical. One difficulty is that generally the ratio decreases as the bubble grows. Here initial values were used to make the classification.

Discussion of Results

The relation betweeen bubble shape, growth rate and surface temperature is readily seen in Figure 2. Shapes and relative sizes of two spherical, one oblate, and one hemispherical bubble are shown after about 1, 2, and 3 msec. of growth. The previous observations at subatmospheric pressure are seen to agree with these atmospheric pressure results. The spherical bubbles are the slowest growing starting at the lowest surface temperature. The hemipsherical bubbles are the fastest growing starting at the highest surface temperature. Oblate bubbles have intermediate growth rates and initial surface temperatures. Values of the radius R, contact diameter, C, surface temperature and microlayer thicknesses M_B and M_T for the four bubbles in Figure 2 are plotted vs. time in Figures 3 to 6.

The average temperature difference, ΔT, which is the average surface thermocouple temperature less the bulk fluid temperature largely correlates with bubble shape but not entirely. Films 32 and 33 had one oblate bubble in each film and many spherical bubbles and had ΔT values shown in Table 1 of 4.5 and 3.0°F., respectively. Films 34, 35, 36, and 37 had more oblate bubbles than spherical bubbles and had ΔT values of 13, 15.3, 13, and 15°F., respectively. Williams' film had only hemispherical bubbles and a ΔT of 26°F. ΔT appears to be a function of the nucleation phenomenon near the surface thermocouple. A better nucleation site should become active at lower temperatures. It was very difficult to get a nucleation site near enough to the thermocouple that the bubble would grow over the thermocouple and yet poor enough to nucleate at a high ΔT. One could sometimes raise the nucleation temperature by repolishing the surface. However, polishing enough to make a difference would usually kill the site.

Microlayer vaporization is most significant in the growth of hemispherical and least significant in spherical bubbles. Examination of values of F_1 and F_2 in Table 2 shows increases from spherical to oblate and from oblate to hemispherical. Bubbles S1 and S2 in Table 2 are actually more spherical than are S3, S4, and S5 and recognizing this increases the value of the comparison. The value of F_1 for bubble H1 in Table 2 is 112.5% but this is questionable. This hemispherical bubble was partially masked by other

TABLE 2. CONTRIBUTION OF MICROLAYER VAPORIZATION FOR BUBBLES OF DIFFERENT SHAPES

Shape of bubble	Bubble and film no.		Delay time* msec.	Initial surface temp., °F.	t_1 msec.	F_1 %	t_2 msec.	F_2 %
spherical	S1	34	0.4	216.8	4.1	7.2	20.2	1.3
	S2	35	0.8	215.0	6.5	3.2	19.8	1.8
	S3	32	1.8	220.4	4.0	18.5	14.6	10.6
	S4	32	4.5	222.6	3.0	34.3	16.6	10.2
	S5	33	7.0	221.7	4.6	25.8	11.4	17.0
oblate	OB1	32	75.0	226.1	3.8	53.4	12.1	31.3
	OB2	33	57.0	224.3	4.5	43.6	12.8	29.2
	OB3	34	77.0	223.0	4.9	49.6	19.4	24.2
	OB4	34	69.0	223.4	4.6	45.6	20.4	19.5
	OB5	35	122.0	221.4	3.1	44.8	17.8	16.8
	OB6	36	264.0	223.4	2.7	51.0	10.4	39.3
	OB7	36	233.0	222.9	3.1	54.4	10.9	42.9
	OB8	37	24.0	223.2	3.9	51.5	13.0	35.3
	OB9	37	24.0	223.3	2.5	38.8	89.8	5.4
	OB10	37	25.0	223.2	2.9	46.0	33.8	18.4
hemispherical	H-1		87.0	231.3	7.4	112.5	—	—

* Time preceding bubble appearance that the position was free of bubbles.

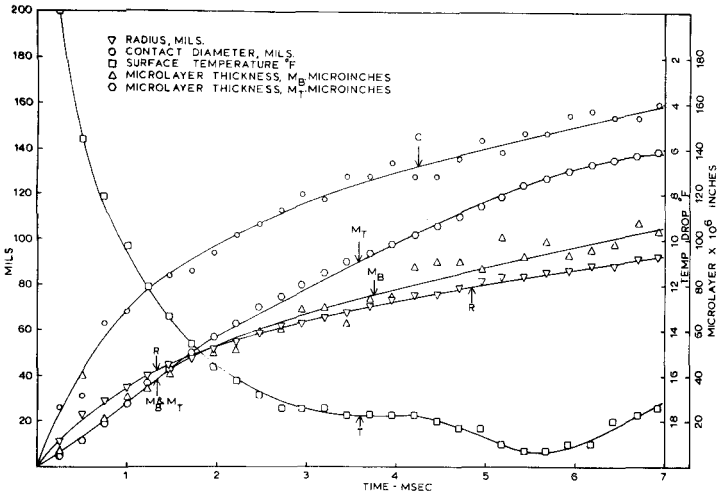

Fig. 6. Plots of radius (*R*), contact diameter (*C*), surface temperature (*T*) and microlayer thickness M_B and M_T for hemispherical bubble *H*1.

bubbles. The bubble shape was judged assuming it to be symmetrical and errors in this procedure may account for the discrepancy. Also, this bubble grew so large it grew out of the field of view. Its volume at detachment could not be accessed so no value for F_2 appears for it. Judging from the trend in F_1 and F_2 values in Table 2, a value of F_2 for H1, would be at least 50%.

As mentioned previously F_2 is a direct measure of microlayer vaporization in latent heat transport. The increase in F_2 to 50% or greater with the more rapidly growing bubbles occurring at the higher surface temperature means microlayer vaporization is the dominant factor in latent transport for these bubbles.

Johnson, de la Pena, and Mesler (*8*) have reported that bubbles which appear soon after a preceding bubble were spherical in shape. The time between the departure of one bubble and the appearance of the next has been described as the delay time. As may be seen in Figures 3 to 9 the surface temperature makes a quick recovery in a few milliseconds from the cooling it experiences during evaporation of the microlayer. Any bubble which grows with a delay of less than a few milliseconds would be growing at a low surface temperature and would therefore tend to be spherical as was reasoned by Johnson, et al. (*8*). Table 2 shows that all the spherical bubbles did have short delay times. Bubbles S1 and S2 were more perfect spheres and their delay times were less than 1 msec. Williams and Mesler (*18*) have observed that artificial nucleation sites especially tend to give small spherical bubbles when boiling on a horizontal surface.

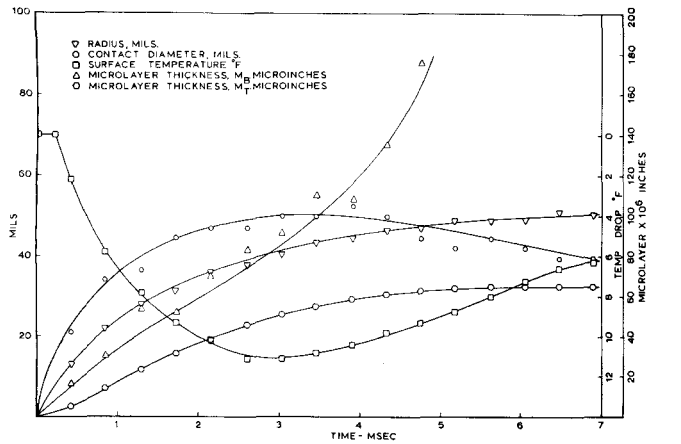

Fig. 7. Plots of radius (*R*), contact diameter (*C*), surface temperature (*T*) and microlayer thickness M_B and M_T for oblate bubble *OB8*.

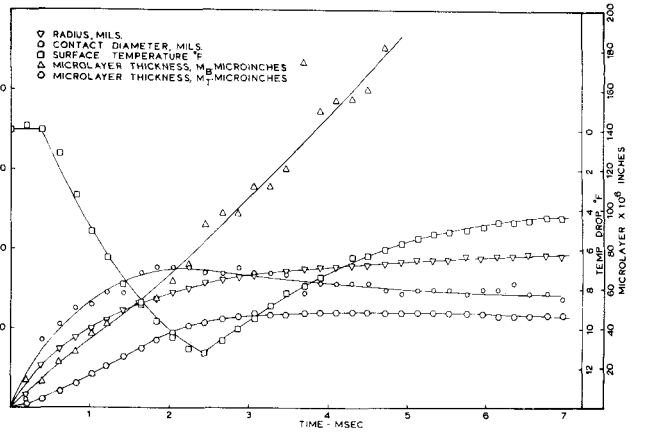

Fig. 8. Plots of radius (*R*), contact diameter (*C*), surface temperature (*T*) and microlayer thickness M_B and M_T for oblate bubble *OB10*.

Initial surface temperature is the more important factor determining bubble growth rate and thus shape. But it is not the only factor. Oblate bubbles OB8, OB10, and OB9, shown in Figures 7, 8, and 9 respectively had the same initial surface temperature and about the same delay time (see Table 2). Bubble OB8 was faster growing than bubble OB10 and OB10 was faster growing than OB9 (see *R* vs. time in plot in Figures 7, 8, and 9). The maximum surface temperature drops for these bubbles OB8, OB10, and OB9 are 11, 11.2 and 7.9°F. respectively at 3, 2.5, and 1.75 msec. respectively. The heat removed at the base of these bubbles progressively decreases in the same order (see plot of M_T vs. time in Figures 7, 8, and 9). Hence, the growth rates of these bubbles progressively decrease. Since the initial surface temperature and delay time for these bubbles of the same film (film 37) were the same, what did influence the growth rate of these bubbles? It was observed that a bubble initiated its growth in the vicinity of the bubble OB9 and there was a vapor mass moving in the bulk of the fluid while OB10 grew on the surface. These disturbances in the neighborhood of the bubble probably influenced the growth rate of these bubbles (OB9 and OB10). It is also interesting to note that the bubble OB9, with a closer disturbance, grew slower compared to the bubble OB10 with the disturbance in the bulk of the fluid. Therefore, there seems to be another factor which influences the growth rate of the bubbles: the agitation or disturbance near the bubbles in addition to the delay time and the initial surface temperature.

Validity of Results

The radius of the bubble, the volume of the bubble and the microlayer thickness M_B were computed using Equa-

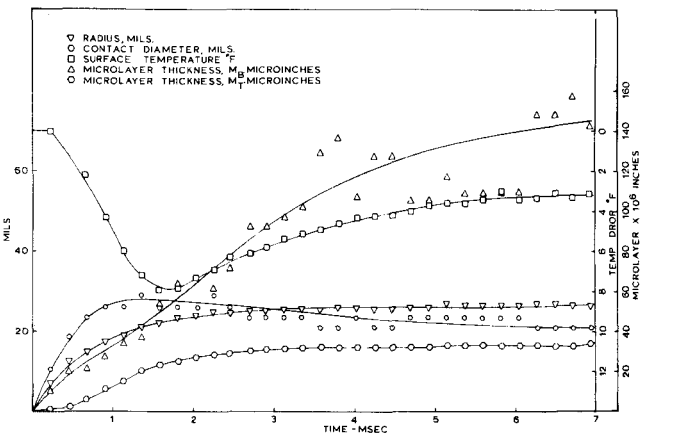

Fig. 9. Plots of radius (*R*), contact diameter (*C*), surface temperature (*T*) and microlayer thickness M_B and M_T for oblate bubble *OB9*.

tions (8), (7), and (9) which assume that the bubble is an oblate spheroid with two axes equal to the maximum width of the bubble.

The maximum errors, involved in measuring A, B, C, and T, were estimated to be $\pm 5\%$. Therefore, the maximum errors involved in computing R, V_B, and M_B would be $\pm 5\%$, $\pm 15\%$, and $\pm 25\%$ respectively utilizing the technique outlined by Mickley, Sherwood, and Reed (*11*).

Rehm (*14*) showed that bubbles are bodies of revolution. This constitutes the basis for assuming that the two axes of the oblate spheroid are equal to A. How accurate is the assumption of an oblate spheroid? A better estimate of the volume of these bubbles was made using the volume integral given by Equation (11).

The percentage error involved in calculating volume from Equation (7) is defined as follows:

$$\% \text{ error} = \frac{V_B - V_B'}{V_B'} \times 100 \qquad (12)$$

During the initial fast growth of the bubbles this error was found to be 9.0% (maximum). But during the detachment stage of the bubble, this error was always positive ranging from 11 to 35%.

The error involved in computing V_B' from Equation (11) was estimated with a few simplifying assumptions (7). This was found to be about $\pm 15.0\%$.

Considering that there could be as much as $\pm 15.0\%$ error in computing V_B' it is reasonable to assume that the bubble is an oblate spheroid during its initial fast growth. But this assumption invariably overestimates the volume of the bubble during the detachment period.

Since V_B and V_D, used to compute F_1 and F_2 were estimated using Equation (11) the errors involved in estimating V_B and V_D could be a maximum of $\pm 15\%$.

The computation of microlayer thickness based on surface temperature, M_T, assumes that the surface temperature variations revealed by the thermocouple represents the entire base of the bubble. In other words, the microlayer thickness is uniform at the base of the bubble. This was indeed shown by Hospeti and Mesler (*5*). It is beyond the scope of this investigation to predict the errors involved in estimating M_T since the accuracy of the assumption involved cannot be predicted.

CONCLUSIONS

1. The growth rate, initial surface temperature, maximum surface temperature drop and bubble volume contribution due to microlayer vaporization at the base of the bubbles, progressively increase for spherical, oblate, and hemispherical bubbles in the same order.

2. In addition to the effects of delay time and initial surface temperature, the agitation in the neighborhood of the bubbles is another factor which appears to influence the growth rate of the bubbles.

ACKNOWLEDGMENT

This research was made possible through a research grant from the National Science Foundation. The computer facilities at the University of Kansas were used extensively. The authors wish to thank Donald Williams for lending one of his high-speed films for our analysis.

NOTATION

A = maximum width of the bubble, mils
B = height of the bubble, mils
C = contact diameter of the bubble, mils
C_p = specific heat B.t.u./(lb.)(°F.)
D = width of the bubble at a height z from the base
F = V_T/V_B
M_B = microlayer thickness based on surface temperafined by Equation (9), microinches
M_T = microlayer thickness based on surface temperature variations defined by Equation (6), microinches
Q/A = integrated heat flux, B.t.u./sq.ft.
R = radius of the bubble, mils
$T(x, t)$ = temperature at a distance x from the surface and at time t, °F.
ΔT = temperature difference between the surface and the bulk fluid at the surface thermocouple
t = time, hr.
V_B = volume of the bubble, cu.in.
V_B' = volume of the bubble computed by D vs. z integration as per Equation (11), cu.in.
V_D = volume of the bubble at the detachment stage, cu.in.
V_T = volume of the vapor formed due to microlayer vaporization defined as per Equation (10)
x = distance from the heat transfer surface, ft.
z = distance from the base of the bubble at which D is measured

Greek Letters

α = thermal diffusivity, sq.ft./hr.
λ = latent heat of water at 212°F. and 14.7 lb./sq.in., B.t.u./lb.
ρ_V = density of water vapor, lb./cu.ft.
ρ_L = density of water, lb./cu.ft.
ρ = density, lb./cu.ft.

Subscripts

1 = at maximum bubble contact
2 = at bubble departure

LITERATURE CITED

1. Bonnet, C., E. Macke, and R. Morin, *EURATOM, Eur. At. Energy Comm., EUR-1622f* (March 1964).
2. Cooper, M. G., and A. J. P. Lloyd, *Proc. 3rd Intern. Heat Transfer Conf.*, **3**, 193, (Aug., 1966).
3. Dergarabedian, P., *J. Appl. Mech.*, **20**, 537 (1953).
4. Hendricks, R. C., and R. R. Sharp, *Nat. Aeron. Space Admin., TN-D-2290* (April, 1964).
5. Hospeti, N. B., and R. B. Mesler, *AIChE J.*, **11**, 662 (1965).
6. ———, *Proc. 7th Intnl. Congr. High-Speed Photography*, Helwich Verlag, Darmstadt, West Germany, pp. 217-221 (1966).
7. Hospeti, N. B., Ph.D. thesis, Univ. Kansas, Lawrence (1966).
8. Johnson, M. A., Jr., J. de la Pena, and R. B. Mesler, *AIChE J.*, **12**, 344 (1966).
9. Kovacs, A., and R. B. Mesler, *Rev. Sci. Inst.*, **35**, 485 (1964).
10. Marcus, B. D., Ph.D. thesis, Cornell Univ., (1963).
11. Mickley, H. S., T. K. Sherwood, and C. E. Reed, "Applied Mathematics in Chem. Eng.," 2nd Ed., p. 57, McGraw Hill, New York (1957).
12. Moore, F. D., M. S. thesis, Univ. Kansas, Lawrence (1960).
13. ———, and R. B. Mesler, *AIChE J.*, **7**, 620 (1961).
14. Rehm, T. R., paper presented at AIChE 55th National Meeting, Houston, Texas (February 1965).
15. Rogers, T. F., and R. B. Mesler, *AIChE J.*, **10**, 656 (1964).
16. Sharp, R. R., *Nat. Aeronaut. Space Admin. TN-D-1997* (Oct., 1964).
17. Strenge, P. R., A. Orell, and J. W. Westwater, *AIChE J.*, **7**, 578 (1961).
18. Williams, D. D., and R. B. Mesler, *ibid.*, **13**, 1020 (1967).
19. Yatabe, J. M., and J. W. Westwater, *Chem. Eng. Progr. Symp. Ser., No. 64*, **62**, 17 (1966).

Manuscript received August 1, 1967; revision received February 19, 1968; paper accepted February 21, 1968. Paper presented at AIChE New York Meeting.